

In this context, adversarial machine learning has appeared as a new branch that aims to thwart intelligent algorithms. Many techniques called adversarial attacks succeeded in fooling well-known architectures of neural networks, sometimes very astonishingly. Examples of these methods include for instance: Fast Gradient Sign Method [7], Basic Iterative Method [10], Projected Gradient Descent [14], JSMA [18], DeepFool [16], Universal Adversarial Perturbations [17] and CW attacks [1].

In this paper, we focus on the following class of attacks:

L_0 (or sparse) adversarial attacks. They aim at generating adversarial samples while minimising the number of modified components. First, many real-life situations may illustrate sparse perturbations. As motivated in [15], *sparse perturbations could correspond to some raindrops that reflect the sun on a “STOP” sign, but that are sufficient to fool an autonomous vehicle; or a crop-field with some sparse colorful flowers that force a UAV to spray pesticide on non affected areas.* Second, sparse perturbations reveal very disturbing and astonishing properties of neural networks such as it is possible to fool them by modifying few pixels [27,15]. Their study is therefore fundamental to mitigate their effects and take a step forward towards robustness of neural networks. The first proposed example of L_0 attacks is JSMA, a targeted attack [18]. In an application to computer vision, JSMA achieved 97% adversarial success rate by modifying in average 4.02% input features per sample. [18] relates this average to the human capability to visually detect changes. An important quality of JSMA is that it is easy to comprehend and set up. In addition, it is relatively fast. For instance, relying on its cleverhans implementation [19], JSMA is able to generate 9 adversarial samples on the MNIST handwritten digits dataset [12] in only 2 seconds on a laptop with 2 CPU cores. Speed and also the ability to run adversarial attacks with limited resources are important criteria for real-life deployment of neural networks [4,6,13]. JSMA obeys to these constraints making its use widespread beyond computer vision applications such as in cybersecurity, anomaly detection and intrusion detection [22,2,23]. Later on, [1] proposes the second example of targeted L_0 attacks known as CW L_0 . The same paper shows that contrary to JSMA, CW L_0 scales well to large datasets by considering the IMAGENET dataset [3]. CW L_0 is now the state-of-the-art L_0 targeted attack in terms of capability to generate adversarial samples and also minimise the L_0 distance. However, it is highly computational, much slower than JSMA on small datasets (a factor of 20 times slower is reported in [1]) and therefore, despite efficiency, it is less convenient for real-time applications.

We summarise our main contributions as follows:

- For targeted misclassification, we introduce two variants of JSMA called Weighted JSMA (WJSMA) and Taylor JSMA (TJSMA). WJSMA applies

a simple penalisation to saliency maps by the output probabilities, while TJSMA applies the same penalisation twice: by the output probabilities and also the input features. Both attacks are more efficient than JSMA according to several metrics (such as speed and mean L_0 distance). We present qualitative and quantitative results on MNIST and CIFAR-10 [8] supporting our claims. Moreover, although they are less efficient than CW L_0 , our attacks have a major speed advantage over this attack highlighted by measuring the execution time for each attack.

- For non-targeted (NT) misclassification, we improve the known NT variants of JSMA called NT-JSMA and Maximal-JSMA (M-JSMA) [29]. We do this by introducing NT and M versions of WJSMA and TJSMA. Our attacks yield better results than NT-JSMA and M-JSMA. Also, they are as competitive but significantly much faster than NT CW L_0 . These claims are illustrated through applications to attack a deep NNC on the GTSRB dataset [26] in the white/black-box modes.
- We provide a deep comparison between WJSMA and TJSMA which is of independent interest. Our study concludes that in the targeted case, TJSMA is more advantageous than WJSMA. However, in the NT case, WJSMA is preferred over TJSMA, mainly due to the simplicity of its implementation.
- We provide fast and optimised implementations of the new attacks using TensorFlow and the `cleverhans` library [19] that might help users working in adversarial machine learning³.

The rest of the paper is organised as follows. Section 2 introduces basic notations and presents a brief review of JSMA and CW L_0 . In Section 3, we discuss our main motivations and then introduce WJSMA and TJSMA as targeted attacks. Section 4 focuses on NT and Maximal versions of WJSMA and TJSMA. Section 5 is dedicated to various experiments and comparisons of our attacks with JSMA and CW L_0 . We discuss attacking, defending with targeted/non-targeted attacks in both the white/black-box modes. Section 6 offers a conclusion and a summary of the main results of the paper. Finally, Section 7 is an appendix dedicated to supplementary results and materials.

2 Notations and review of JSMA and L_0 CW attacks

The goal of a Neural network classifier (NNC) is to predict through a neural network which class an item x belongs to, among a family of K possible classes.

³In all our experiments, we use the original implementation of JSMA available in the `cleverhans` library and the original code of CW publicly available. As for the NT versions of JSMA [29], whose implementations are not available, we re-implement these attacks using TensorFlow and `cleverhans`.

It outputs a vector of probabilities $F(x) = (F_1(x), \dots, F_K(x))$ where the label of x is deduced by the rule $\text{label}(x) = \text{argmax}_k F_k(x)$.

JSMA. To fool NNCs, this attack relies on the Jacobian matrix of outputs with respect to inputs. By analysing this matrix, one can deduce how the output probabilities behave given a slight modification of an input feature. Consider a NNC N as before and call $Z(x) = (Z_1(x), \dots, Z_K(x))$ the outputs of the second-to-last layer of N (no longer probabilities, but related to the final output by a softmax layer). To generate an adversarial example from x , JSMA first computes the gradient $\nabla Z(x)$. The next step is constructing a saliency map whose function is to select the most salient component i to perturb:

$$S[x, t][i] = \begin{cases} 0 & \text{if } \frac{\partial Z_t(x)}{\partial x_i} < 0 \text{ or } \sum_{k \neq t} \frac{\partial Z_k(x)}{\partial x_i} > 0 \\ \frac{\partial Z_t(x)}{\partial x_i} \cdot \left| \sum_{k \neq t} \frac{\partial Z_k(x)}{\partial x_i} \right| & \text{otherwise.} \end{cases} \quad (1)$$

The role of $\frac{\partial Z_t(x)}{\partial x_i}$ and $\sum_{k \neq t} \frac{\partial Z_k(x)}{\partial x_i}$ in these maps is to increase $Z_t(x)$ and decrease $\sum_{k \neq t} Z_k(x)$. Counting on the Z_k 's instead of the F_k 's has been justified in [18] by the extreme variations induced by the logistic regression. Then the algorithm selects the component: $i_{\max} = \text{argmax}_i S[x, t][i]$ and augments $x_{i_{\max}}$ with a default increase value θ before clipping to the valid domain. The same process is iterated until changing the class of x or reaching a maximum allowed number of iterations. This version of JSMA will be called one-component. A second, more effective, variant of JSMA recalled later relies on doubly indexed saliency maps.

CW L_0 attack. This method is obtained as a solution to the optimisation problem (assuming the domain of inputs is $[0, 1]^n$):

$$\text{Minimise } \|r\|_0 + cf(x + r), \quad x + r \in [0, 1]^n$$

where $\|r\|_0$ is the L_0 distance of the perturbation r added to x . The recommended choice of f is: $f(x) = (\max_{i \neq t} Z_i(x) - Z_t(x))^+$. Since the L_0 distance is not convenient for a gradient descent, the authors of [1] solve the previous problem by making use of their L_2 attack and an algorithm that iteratively eliminates the components with no much effect on the output classification. They finally obtain an effective L_0 attack that has net advantage over JSMA. The main drawback of this attack is however its highly computational cost.

3 Targeted attacks

The first attacks, presented in this section, are targeted and called Weighted JSMA and Taylor JSMA (TJSMA). We give a detailed exposition of WJSMA and motivate the main idea leading to its derivation through a simple example. Then, we deduce TJSMA by applying once more and in a slightly different manner the same argument. In addition to the theoretical presentation, few preliminary figures are given to illustrate a faster convergence of the new attacks in comparison with JSMA.

3.1 Weighted Jacobian-based Saliency Map Attack (WJSMA)

The main idea here is to penalise gradients associated with small probabilities so as to mitigate their influences in saliency maps. The goal is to obtain more balanced saliency maps than those proposed by JSMA. We first give a concrete example illustrating a concrete limitation of JSMA which motivated this work.

Motivating example. Assume a number of classes $K \geq 4$ and for some input x : $F_1(x) = 0.5$, $F_2(x) = 0.49$, $F_3(x) = 0.01$ and $F_k(x) = 0$ for all $4 \leq k \leq K$. Consider the problem of generating an adversarial sample to x with label $t = 2$. In order to decrease $\sum_{k \neq 2} Z_k(x)$, the first iteration of JSMA

relies on the gradients $\nabla Z_k(x)$, $k \neq 2$. Our main observation is that since the probabilities $F_k(x) = 0$ for $4 \leq k \leq K$ are already in their minimal values, taking into account $\nabla Z_k(x)$ for these values of k in the search of i_{\max} is unnecessary. In other words, by only acting on gradients, JSMA does not consider the crucial constraints on probabilities: $F_k(x) \geq 0$. Moreover, instead of relying equally on $\nabla Z_1(x)$ and $\nabla Z_3(x)$, for this example one would “bet more” on $\nabla Z_1(x)$ than $\nabla Z_3(x)$ as the possible decrease for $F_1(x)$ is high (up to 0.5) and $F_3(x)$ is relatively small, thus hard to decrease further.

Weighted JSMA (WJSMA). Our first solution to the previous issue is WJSMA. Its principle is to penalise each gradient $\frac{\partial Z_k(x)}{\partial x_i}$, where $k \neq t$, by the probability $F_k(x)$. Besides the intuition of this idea, we will provide a justification of it by a classical log softmax argument. First, we compute:

$$\frac{\partial}{\partial x_i} \log F_t(x) = (1 - F_t(x)) \frac{\partial Z_t}{\partial x_i}(x) - \sum_{k \neq t} F_k(x) \frac{\partial Z_k}{\partial x_i}(x)$$

One way to maximise this derivative with respect to i , is to maximise $A = \frac{\partial Z_t}{\partial x_i}(x)$ and minimise $B = \sum_{k \neq t} F_k(x) \frac{\partial Z_k}{\partial x_i}(x)$ under the constraints $A > 0$

and $B < 0$. These constraints ensure, in particular, that $\frac{\partial F_t}{\partial x_i}(x)$ remains positive, a fact which is not necessarily guaranteed under JSMA constraints. According to this, we introduce one-component weighted saliency maps as follows:

$$S^W[x, t][i] = \begin{cases} 0 & \text{if } \frac{\partial Z_t(x)}{\partial x_i} < 0 \text{ or } \sum_{k \neq t} F_k(x) \frac{\partial Z_k(x)}{\partial x_i} > 0 \\ \frac{\partial Z_t(x)}{\partial x_i} \cdot \left| \sum_{k \neq t} F_k(x) \frac{\partial Z_k(x)}{\partial x_i} \right| & \text{otherwise.} \end{cases}$$

Based on these maps, we present Algorithm 1, the first version of WJSMA to generate targeted adversarial samples.

Algorithm 1 Generating adversarial samples by WJSMA: version 1

Inputs: N : a NNC, Z : second-to-last output of N , x : input to N , t : target label ($t \neq \text{class}(x)$), **maxIter**: maximum number of iterations, $\theta_{\min}, \theta_{\max}$ lower and upper bounds for features values, θ : positive default increase value.

Output: x^* : adversarial sample to x .

```

 $x^* \leftarrow x$ 
iter  $\leftarrow 0$ 
 $\Gamma \leftarrow \llbracket 1, |x| \rrbracket \setminus \{p \in \llbracket 1, |x| \rrbracket \mid x[p] = \theta_{\max}\}$ 
while  $\text{class}(x^*) \neq t$  and iter  $<$  maxIter and  $\Gamma \neq \emptyset$  do
     $p_{\max} = \text{argmax}_{p \in \Gamma} S^W[x^*, t](p)$ 
    Modify  $x^*$  by  $x^*[p_{\max}] = \text{Clip}_{[\theta_{\min}, \theta_{\max}]}(x^*[p_{\max}] + \theta)$  //Clip is the clipping function
    Remove  $p_{\max}$  from  $\Gamma$ 
    iter ++
end while
return  $x^*$ 

```

When the output x^* of Algorithm 1 satisfies $\text{class}(x^*) = t$, the attack is considered as successful.

To relax a bit the search of salient components and motivated by a computer vision application, [18] introduces saliency maps indexed by pairs of components. The main argument is that the conditions required in (1) may be too severe for some applications and very few components will verify it. Our doubly

indexed versions of these maps are introduced in the same way as follows:

$$S^W[x, t][i, j] = \begin{cases} 0 & \text{if } \sum_{a \in \{i, j\}} \frac{\partial Z_t(x)}{\partial x_a} < 0 \text{ or } \sum_{k \neq t} F_k(x) \sum_{a \in \{i, j\}} \frac{\partial Z_k(x)}{\partial x_a} > 0 \\ \sum_{a \in \{i, j\}} \frac{\partial Z_t(x)}{\partial x_a} \cdot \left| \sum_{k \neq t} F_k(x) \sum_{a \in \{i, j\}} \frac{\partial Z_k(x)}{\partial x_a} \right| & \text{otherwise.} \end{cases} \quad (2)$$

Algorithm 2 presented below relies on $S^W[x, t][i, j]$ to generate targeted adversarial samples and is our second version of WJSMA.

Algorithm 2 Generating adversarial samples by WJSMA: version 2

Same inputs and output as Algorithm 1.

```

 $x^* \leftarrow x$ 
iter  $\leftarrow 0$ 
 $\Gamma \leftarrow \{(p, q), p, q \in \llbracket 1, |x| \rrbracket, x[p] \neq \theta_{max}, x[q] \neq \theta_{max}\}$ 
while class( $x^*$ )  $\neq t$  and iter  $<$  maxIter and  $\Gamma \neq \emptyset$  do
    ( $p_{max}, q_{max}$ ) = argmax $_{p, q \in \Gamma} S^W[x^*, t](p, q)$ 
    Modify  $x^*$  by  $x^*[a] = \text{Clip}_{[\theta_{min}, \theta_{max}]}(x^*[a] + \theta)$ ,  $a = p_{max}, p_{max}$ 
    Remove ( $p_{max}, q_{max}$ ) from  $\Gamma$ 
    iter ++
end while
return  $x^*$ 

```

In practice and despite the fact that Algorithm 2 is more computational, we find that it gives better results than Algorithm 1. This agrees with the recommendations of [18] on the superiority of two-components versions for JSMA. Finally, we notice that while in the two previous algorithms, the selected components are always augmented by positive default values, decreasing versions can be given following a similar logic.

3.2 Taylor Jacobian-based Saliency Map Attack (TJSMA)

The principle of our second proposed attack TJSMA is to additionally penalise the choice of feature components that are close to the maximum value θ_{max} . Assume i and j have the same WJSMA score $S^W[x, t][i] = S^W[x, t][j]$ and that x_i is very close to, while x_j is far enough from θ_{max} . In this case, searching for more impact, TJSMA prefers x_j over x_i . Concretely, we simultaneously maximise $S_1 = \theta_{max} - x_i$ and $S_2 = \frac{\partial}{\partial x_i} \log p_t(x)$ by maximising the product

$S = S_1 S_2$. Accordingly, we introduce new saliency maps for one and two-components selection as follows:

$$S^T[x, t][i] = \begin{cases} 0 & \text{if } \alpha_i < 0 \text{ or } \beta_i > 0 \\ |\alpha_i| |\beta_i| & \text{otherwise.} \end{cases} \quad (3)$$

where

$$\alpha_i = (\theta_{\max} - x_i) \frac{\partial Z_t(x)}{\partial x_i}, \quad \beta_i = (\theta_{\max} - x_i) \sum_{k \neq t} F_k(x) \frac{\partial Z_k(x)}{\partial x_i}$$

and

$$S^T[x, t][i, j] = \begin{cases} 0 & \text{if } \alpha_{i,j} < 0 \text{ or } \beta_{i,j} > 0 \\ |\alpha_{i,j}| |\beta_{i,j}| & \text{otherwise.} \end{cases} \quad (4)$$

where

$$\alpha_{i,j} = \sum_{a \in \{i,j\}} (\theta_{\max} - x_a) \frac{\partial Z_t(x)}{\partial x_a}, \quad \beta_{i,j} = \sum_{k \neq t} \sum_{a \in \{i,j\}} F_k(x) (\theta_{\max} - x_a) \frac{\partial Z_k(x)}{\partial x_a}$$

Due to the presence of the Taylor terms $(\theta_{\max} - x_a) \frac{\partial Z_k(x)}{\partial x_a}$, we call these maps Taylor saliency maps. We introduce one and two-components TJ SMA following exactly Algorithms 1, 2 and only replacing S^W with S^T .

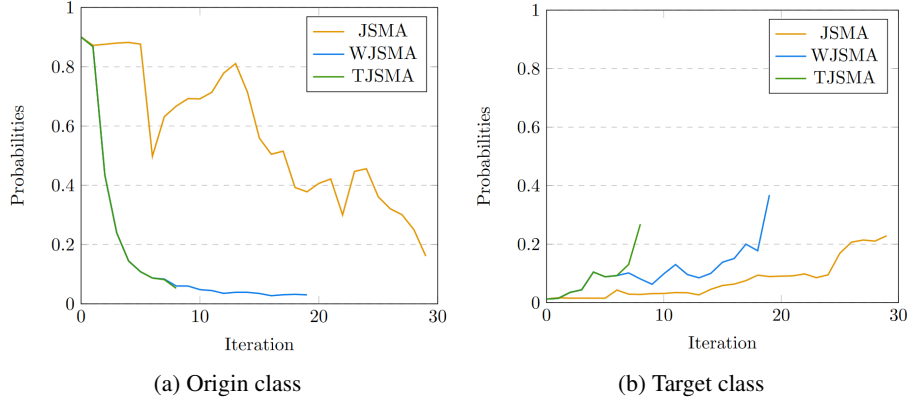


Fig. 1: Evolution of the origin and target class probabilities until the target class is reached for JSMA, WJSMA and TJSMA changing the image of a one into a five.

Figures 1a and 1b offer a concrete illustration of the convergence of JSMA, WJSMA and TJSMA. In particular, we observe that WJSMA and TJSMA decrease/increase the predicted/targeted probability of the original/targeted class much sooner than JSMA. Also, we note that TJSMA behaves like WJSMA until it is able to find a more vulnerable component that makes it converge much faster.

4 Non-targeted attacks

NT variants of JSMA have been studied in [29]. In particular, the paper introduces NT-JSMA-F, NT-JSMA-Z based on NT saliency maps whose role is to select the most salient pairs of components to decrease at most the probability of the current class. The notations -F and -Z indicate if the saliency maps either use the F_k 's or the Z_k 's. Second, [29] proposes maximal JSMA (M-JSMA) as a more flexible attack allowing both increasing/decreasing features and also combining targeted/non-targeted strategies at the same time.

In what follows, we again leverage the idea of penalising saliency maps to give our proper NT JSMA attacks. For a unified presentation, we use the letter X to denote either W (Weighted) or T (Taylor) and the letter Y to denote either Z (logits) or F (probabilities). We notice that while the first version of JSMA uses the logits, variants that rely on the F_k 's also demonstrated good performances [1,29]. Thus for a more complete study, we give versions with both Z and F .

By a NT reasoning analogous to the previous section, we define Weighted and Taylor NT saliency maps as follows:

$$S^{X,Y}[x, t][i, j] = \begin{cases} 0 & \text{if } \alpha_{i,j}^{X,Y} > 0 \text{ or } \beta_{i,j}^{X,Y} < 0 \\ |\alpha_{i,j}^{X,Y}| |\beta_{i,j}^{X,Y}| & \text{otherwise.} \end{cases} \quad (5)$$

where, for $X = W$,

$$\alpha_{i,j}^{W,Y} = \sum_{a \in \{i,j\}} \frac{\partial Y_t(x)}{\partial x_a}, \quad \beta_{i,j}^{W,Y} = \sum_{k \neq t} \sum_{a \in \{i,j\}} F_k(x) \frac{\partial Y_k(x)}{\partial x_a}$$

and, for $X = T$,

$$\alpha_{i,j}^{T,Y} = \sum_{a \in \{i,j\}} (\theta_{\max} - x_a) \frac{\partial Y_t(x)}{\partial x_a}, \quad \beta_{i,j}^{T,Y} = \sum_{k \neq t} \sum_{a \in \{i,j\}} F_k(x) (\theta_{\max} - x_a) \frac{\partial Y_k(x)}{\partial x_a}$$

These maps can be motivated as the previous section by considering the simple case of one-component: $i = j$. For example, the role of the penalisation

by $F_k(x)$ in $S^{W,Z}$ is to reduce the impact of high gradients $\frac{\partial Z_k(x)}{\partial x_i}$ when the probability $F_k(x)$ is very small (in this case we penalise choosing k as a new target for x).

Relying on saliency maps, Algorithm 2 below presents our improvements of NT-JSMA-Z and NT-JSMA-F. For the sake of simplification, we have employed a unified notation NT-XJSMA-Y. For example, when we use $S^{W,Z}$, the obtained attack is NT-WJSMA-Z. Again, we only write the increasing version.

Algorithm 3 NT-WJSMA and NT-TJSMA attacks

Inputs: x : input to N with label t , maxIter : maximum number of iterations, $X \in \{W, T\}$, $Y \in \{Z, F\}$

Output: x^* : adversarial sample to x .

```

 $x^* \leftarrow x$ 
 $\text{iter} \leftarrow 0$ 
 $\Gamma \leftarrow \{(p, q), p, q \in \llbracket \theta_{\max}, |x| \rrbracket, x[p] \neq \theta_{\max}, x[q] \neq \theta_{\max}\}$ 
while  $\text{class}(x^*) \neq t$  and  $\text{iter} < \text{maxIter}$  and  $|\Gamma| \geq 2$  do
     $(p_{\max}, q_{\max}) = \text{argmax}_{p, q \in \Gamma} S^{X, Y}[x^*, t](p, q)$ 
    Modify  $x^*$  by  $x^*[p_{\max}], x^*[q_{\max}] = \theta_{\max}$ 
    Remove  $(p_{\max}, q_{\max})$  from  $\Gamma$ 
     $\text{iter} ++$ 
end while
return  $x^*$ 

```

We now turn to extensions of M-JSMA [29]. This attack modifies the pairs of components achieving the best score among NT-JSMA and all possible targeted (including increasing and decreasing) JSMA. It has more ability to craft adversarial samples but is relatively slower than NT-JSMA. Our extensions of M-JSMA, which we call M-WJSMA and M-TJSMA, are described in Algorithm 4.

Note that saliency maps $S^{W, Y}$ for targeted, non-targeted, features increasing or features decreasing attacks are exactly the same (one only needs to decide between an argmax or argmin). This is not the case for M-TJSMA since for example $(\theta_{\max} - x_a)$ has to be changed to $x_a - \theta_{\min}$ when decreasing features. As a consequence of this fact, M-WJSMA is less cumbersome to implement than M-TJSMA. Trying to keep the paper and code as simple as possible, we chose to prefer M-WJSMA over M-TJSMA and not include M-TJSMA in our experiments. We notice that M-WJSMA already gives us satisfactory results.

Algorithm 4 M-WJSMA and M-TJSMA attack

Inputs: x : input to N with label t , maxIter : maximum number of iterations, $X \in \{W, T\}$, $Y \in \{Z, F\}$

Output: x^* : adversarial sample to x .

```
 $x^* \leftarrow x$ 
iter  $\leftarrow$  0
 $\Gamma \leftarrow \{(p, q), p, q \in \llbracket 1, |x| \rrbracket, x[p], x[q] \neq \theta_{\min}, \theta_{\max}\}$ 
while  $\text{class}(x^*) \neq t$  and iter  $<$   $\text{maxIter}$  and  $|\Gamma| \geq 2$  do
  - Compute all targeted increasing/decreasing saliency maps scores  $S^{X,Y}[x, s](p, q)$ ,  $s \neq t$ 
  (Section 3) and all NT increasing/decreasing saliency maps scores  $S^{X,Y}[x, t](p, q)$  (5).
  - Choose  $(p_{\max}, q_{\max})$  achieving the best score and saturate  $x^*[p_{\max}]$ ,  $x^*[q_{\max}]$  to  $\theta_{\min}$  or  $\theta_{\max}$ 
  according to the chosen saliency map.
  - Remove  $(p_{\max}, q_{\max})$  from  $\Gamma$ 
  - iter ++
end while
return  $x^*$ 
```

5 Experiments

This section is dedicated to a variety of experiments on the proposed attacks and several comparisons with the state-of-the-art methods. The first part focuses on targeted attacks and provides intensive comparisons between JSMA, WJSMA and TJSMA on deep NNCs on MNIST and CIFAR-10 as well as comparisons with CW L_0 . In the second part, we show that our approach is still relevant for non-targeted L_0 misclassification in both the white-box and black-box modes. A particular emphasis will be put on the speed of our attacks in comparison with CW L_0 .

5.1 Experiments on targeted attacks

In the following, we give attack and defense applications illustrating the interest of WJSMA and TJSMA over JSMA. In doing so, we also compare WJSMA and TJSMA and report overall better results for TJSMA despite the fact that for a large part of samples WJSMA outperforms TJSMA. Finally, we provide a comparison with CW L_0 attack and comment on all the obtained results.

The datasets used in this section are:

MNIST [12]. This dataset contains 70,000 28×28 greyscale images in 10 classes, divided into 60,000 training images and 10,000 test images. The possible classes are digits from 0 to 9.

CIFAR-10 [8]. This dataset contains 60,000 $32 \times 32 \times 3$ RGB images. There are 50,000 training images and 10,000 test images. These images are divided

into 10 different classes (airplane, automobile, bird, cat, deer, dog, frog, horse, ship, truck), with 6,000 images per class.

Figures 2 and 3 display one sample per class, from MNIST and CIFAR-10 respectively.



Fig. 2: Examples of images from MNIST



Fig. 3: Examples of images from CIFAR-10

On each dataset, a deep NNC is trained and then subjected to attacks.

NNC on MNIST. Similarly to [18], we consider LeNet-5 model on this dataset [11]. Its full architecture is described in the appendix. We implement and train this model using a `cleverhans` model that optimises crafting adversarial examples. The number of epochs is fixed to 20, the batch-size to 128, the learning rate to 0.001 and the Adam optimizer is used. Training results in a 100% accuracy on the training dataset and 99.49% accuracy on the test dataset.

NNC on CIFAR-10. We consider a more complex NNC trained to reach a good performance on this dataset. Its architecture is inspired by the AllConvolutional model proposed in `cleverhans` and is fully described in the appendix. Likewise, this model is implemented and trained using `cleverhans` for 10 epochs, with a batch size of 128, a learning rate of 0.001 and the Adam optimizer. Training results in a 99.96% accuracy on the training dataset and 83.81% accuracy on the test dataset.

Our first objective is to compare the performances of JSMA, WJSMA and TJSMA on the previous two NNC. To run JSMA, we use its original implementation available in `cleverhans`. We have also adapted the code to WJSMA and TJSMA thus obtaining fast implementations of these two attacks.

For testing, we consider all images in MNIST, the first 10, 000 training and 10, 000 test images of CIFAR-10. Moreover, we only test on the images which

are correctly predicted by the neural networks as this makes more sense. In this way, the attacks are applied to the whole training set and the 9,949 well-predicted images of the MNIST test images. Similarly, CIFAR-10 adversarial examples are crafted from the well-predicted 9,995 images of the first training 10,000 images and the 8,381 well-predicted test images.

To compare the three attacks, we rely on the notion of maximum distortion of adversarial samples defined as the ratio of altered components to the total number of components. Following [18], we choose a maximum distortion of $\gamma = 14.5\%$ on the adversarial samples from MNIST, corresponding to $\text{maxIter} = \lfloor \frac{784 * \gamma}{2 * 100} \rfloor$. On CIFAR-10, we fix $\gamma = 3.7\%$ in order to have the same maximum number of iterations for both experiments. This allows a comparison between the attacks in two different settings. Furthermore, for both experiments, we set $\theta = 1$ (note that $\theta_{\min} = 0$, $\theta_{\max} = 1$).

We report the metrics:

- (1) Success rate: This is the percentage of successful adversarial examples, i.e crafted before reaching the maximal number of iterations `maxIter`,
- (2) Mean L_0 distance: This is the average number of altered components of the successful adversarial examples,
- (3) Strict dominance of an attack: Percentage of adversarial examples for which this attack does strictly less iterations than the two other ones⁴,
- (4) Run-time of an attack on a set of samples targeting every possible class.

Results on the metrics (1) and (2) are shown in Table 1 for MNIST and Table 2 for CIFAR-10.

Table 1: Comparison between JSMA, WJSMA and TJSMA on MNIST.

Metric	JSMA	WJSMA	TJSMA
Targeted (Training dataset: Nb of well predicted images=60,000)			
Success rate	87.68%	97.14%	98.66%
Mean L_0 distance on successful samples	44.34	37.86	35.22
Targeted (Test dataset: Nb of well predicted images=9,949)			
Success rate	87.34%	96.98%	98.68%
Mean L_0 distance on successful samples	44.63	38.10	35.50

⁴ As additional results, we give in the appendix more statistics on the dominance between any two attacks.

Table 2: Comparison between JSMA, WJSMA and TJSMA on CIFAR-10.

Metric	JSMA	WJSMA	TJSMA
Targeted (Training dataset: Nb of well predicted images=9 995)			
Success rate	86.17	95.91%	97.40%
Mean L_0 distance on successful samples	47	38.54	36.86
Targeted (Test dataset: Nb of well predicted images=8 381)			
Success rate	84.91	94.99%	96.96%
Mean L_0 distance on successful samples	46.13	38.82	37.45

First, we observe that overall, WJSMA and TJSMA significantly outperform JSMA according to the metrics (1)-(2). Here, are more comments:

On MNIST. Results in terms of success rate are quite remarkable for WJSMA and TJSMA respectively outperforming JSMA with near 9.46, 10.98 percentage points (pp) on the training set and 9.46, 11.34 pp on the test set. The gain in the average number of altered components exceeds 6 components for WJSMA and 9 components for TJSMA in both experiments.

On CIFAR-10. WJSMA and TJSMA outperform JSMA in success rate by near 9.74, 11.23 pp on the training set and more than 10, 12 pp on the test set. For both training and test sets, we report better mean L_0 distances exceeding 7 features in all cases and up to 10.14 features for TJSMA on the training set.

Dominance of the attacks. The next figures illustrate the (strict) dominance of the attacks for the two experiments. In these statistics, we do not count the samples for which TJSMA and WJSMA realise the same number of iterations strictly less than JSMA.

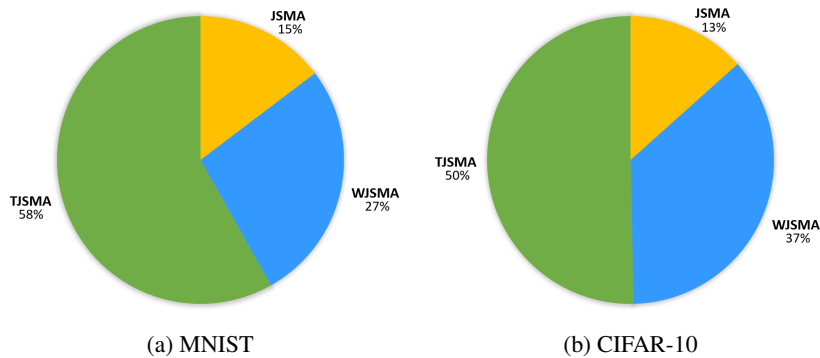


Fig. 4: Distribution of the (strict) dominance of JSMA, WJSMA and TJSMA over the MNIST and CIFAR10 datasets (training and test sets included)

For both experiments, TJSMA has a notable advantage over WJSMA and JSMA. The benefit of WJSMA over JSMA is also considerable. This shows that, in most cases, WJSMA and TJSMA craft better adversarial examples than JSMA, while being faster. Our results are indeed better when directly comparing WJSMA or TJSMA with JSMA. As additional results, we give in the appendix the statistics for the pairwise dominance between the attacks. As it might be expected, both WJSMA and TJSMA dominate JSMA, moreover TJSMA dominate WJSMA.

Avoid confusion. It is important to stress that our results do not contradict [18] obtaining 97% success rate on LeNet-5. Indeed, we use a more efficient LeNet-5 model (the one in [18] has 98.93% and 99.41% accuracies on the training and test sets). For completeness, we also generated a second model (with 99.34% and 98.94% accuracies on the training and test sets) and evaluated the three attacks on the first 1,000 test MNIST images. We obtain 96.7% success rate for JSMA (very similar to [18]) and more than 99.5% for WJSMA and TJSMA. We preferred to work with the more effective model as this makes the paper shorter and moreover it values more our approach (giving us more advantage with respect to JSMA).

Run-time comparison. In order to have a meaningful speed comparison between the three attacks, we computed the time needed for each attack to successfully craft the first 1,000 test MNIST images in the targeted mode. Results are shown in Table 5 and reveal that TJSMA/WJSMA are 1.41/1.28 times faster than JSMA. These performance tests were realised on a machine equipped with an Intel Xeon 6126 processor and a Nvidia Tesla P100 graphics processor. Note that for WJSMA/TJSMA, the additional computations of one iteration compared to JSMA are negligible (simple multiplications). Thus the difference in speed between the attacks is mainly due to the number of iterations for each attack.

Table 3: Time comparison between JSMA, WJSMA and TJSMA

Attack	JSMA	WJSMA	TJSMA
Time (second)	3964	3092	2797

We also notice that in this evaluation, the adversarial samples were crafted one by one. In practice, it is possible to generate samples by batch. In this case,

the algorithm stops when all samples are finished. Most of the time, with a batch of large size, the three attacks approximately take the same time to converge. For example, on the same machine as previously and with a batch size equal to 1000, we were able to craft the same amount of samples in about 250s, for all the attacks.

Defense. The objective now is to train neural networks in a way that the attacks fail as much as possible. One way of doing this is by adding adversarial samples crafted by JSMA, WJSMA and TJSMA to the training set. This method of training may imply a decrease in the model accuracy but adversarial examples will be more difficult to generate.

We experiment this idea on the MNIST model in every possible configuration. To this end, 2,000 adversarial samples per class (20,000 more images in total), with distortion under 14.5%, are added to the original MNIST training set, crafted by either JSMA, WJSMA or TJSMA. Then, three distinct models are trained on these augmented datasets. The models roughly achieve an accuracy of 99.9% on the training set and 99.3% on the test set, showing a slight loss compared to our previous MNIST model. Nevertheless, the obtained neural networks are more robust to the attacks as shown in Table 4. Note that each experiment is made over the well-predicted samples of the test images. For each model and image, nine adversarial examples are generated by the three attacks.

Table 4: Metrics (1) and (2) on JSMA, WJSMA and TJSMA augmented sets

Metric	JSMA	WJSMA	TJSMA
Model trained over JSMA augmented set (9940 well predicted samples)			
Success rate	77.94%	84.79%	85.08%
Mean L_0 distance on successful samples	54.48	52.66	52.83
Model trained over WJSMA augmented set (9936 well predicted samples)			
Success rate	77.61%	90.05%	92.01%
Mean L_0 distance on successful samples	56.29	52.72	52.18
Model trained over TJSMA augmented set (9991 well predicted samples)			
Success rate	76.42%	86.18%	87.36%
Mean L_0 distance on successful samples	54.26	54.20	54.49

Overall, the attacks are less efficient on each of these models, compared to Table 1. The success rates drop by about 8 pp, whereas the number of iterations is increased by approximately 26%. From the defender’s point of view, networks trained against WJSMA and TJSMA give the best performance. The

JSMA trained model provides the lowest success rates while the TJSMA trained network is more robust from the L_0 distance point of view. From the attacker’s point of view, TJSMA remains the most efficient attack regardless of the augmented used dataset.

Comparison with CW L_0 attack. Because of the complexity of this attack, comparison on a large amount of images as before is so costly. For this reason, we only provide results on the first 100 well-predicted images of CIFAR-10, thus on 1, 000 adversarial images given in Table 5.

Table 5: Results for L_0 CW on CIFAR-10

Success rate	Mean L_0 distance	Time
99.89%	24.97	In average more than one hour and a half to generate 9 adversarial samples run one by one on GPU

We report better results of CW in terms of success rate and L_0 distance and a very remarkable speed advantage of our attacks. Indeed, generating 9 adversarial samples (one by one) from a CIFAR-10 image by CW took in average near one hour and a half on GPU. The same task took 100 seconds for our attacks (without batching and 25 seconds when batching). This makes our attacks at least 54 times faster than CW L_0 .

5.2 Experiments on non-targeted attacks

In this part, we test the new NT attacks in the white/black-box modes and compare their performances with NT-JSMA and M-JSMA. In the white-box mode, we also compare with NT CW L_0 . For experimentation, we chose the GTSRB dataset [26] widely used to challenge neural networks especially in autonomous driving environments [20]. We recall that GTSRB contains RGB $32 \times 32 \times 3$ traffic signs images, 86989 in the training set, and 12630 in the test set classified into 43 different possible categories. Figure 5 displays some images from this dataset.



Fig. 5: Examples of images from GTSRB

5.3 White-box experiments

We consider a simplified NNC, described in the appendix, whose architecture is inspired by Alexnet [9]. After training this model with `cleverhans`, it reaches 99.98% accuracy on the training dataset and 95.83% accuracy on the test set.

We implemented our attacks and those of [29] again with TensorFlow using `cleverhans`. During the first experiment, we run the attacks given in Table 6 on the first 1, 000 test images after taking a maximum distortion $\gamma = 3.7\%$ similar to CIFAR-10. The obtained results are shown in the same table.

Attack (U=JSMA)	Success rate	L_0 average	Time (sec)
NT-U	91.35%	20.66	3604
NT-WU (ours)	95.31%	17.63	760
NT-TU (ours)	96.87%	15.86	660
M-U	98.44%	18.99	7470
M-WU (ours)	99.37%	15.52	6302
CW L_0	97.81%	13.56	260751

Table 6: Comparison of the performances between the NT attacks over the 1, 000 first test images of GTSRB.

To analyse these results, it makes more sense to separately compare the NT-versions (faster), the M-versions (the most effective in success rate but slower) and discuss a global comparison with CW L_0 . First, we notice a significant advantage of our NT versions over NT-JSMA according to the three metrics. In particular NT-TJSMA is up to $5.4\times$ faster than NT-JSMA with nearly 4.8 less modified pixels in average and more than 5 percentage points in success rate. We also remark that NT-TJSMA is the most effective attack among the three NT versions. Its notable benefit over NT-WJSMA is due to the fact that it performs few less iterations than NT-WJSMA while both attacks need approximately the same time for an iteration. As for the M-versions, our attack M-WJSMA outperforms M-JSMA according to the three reported metrics. Both attacks are

however slower than the NT versions. Finally, we remark that the gap between our attack M-WJSMA and CW L_0 is reduced as we obtain better success rate, achieve less than two pixels in L_0 average while being more than 40 times faster.

5.4 Black-box experiments

Here, we consider that black-box attack means the algorithm can use the targeted model as an oracle : when feeding it an image, the oracle returns a single class label. Moreover, we want to make only a limited amount of queries, which in a realistic setup would mean avoiding any suspect activity, or at least trying not to depend too much on the oracle. To overcome this restriction, we train a substitute NNC using the Jacobian-based Dataset Augmentation (JBDA) [20] method. We then perform white-box attacks on the substitute NNC. If it is good enough, the resulting adversarial images should *transfer* to the oracle, i.e. effectively fool it even though they were designed to fool the substitute. Details about the substitute NNC architecture can be found in the appendix. The JBDA method allows us to make queries to the oracle only during the training of the substitute network. Black-box attacks are thus closer to real-life setups, as one only needs to access for a short period of time to the targeted model before being able to durably fool it. A dangerous application of such techniques is against autonomous driving cars and their sign recognition systems. NT black-box attacks are exactly the kind of threat that can be put in practice with relative ease and still disrupt considerably the car’s behaviour. We will illustrate this insecurity through the GTSRB dataset.

Attacks in this paragraph are NT-JSMA and M-JSMA [29], along with our contribution NT-WJSMA, NT-TJSMA and M-WJSMA. We experiment with different distortion rates. Contrary to white-box attacks, in the context of black-box attacks, the distortion rate is not an upper bound on the percentage of pixels that can be modified, but the exact percentage of pixels we want to perturb. This slight difference accounts for the imperfection of the substitute network : even if it mimics quite well the oracle, stopping as soon as the image switches according to the substitute will often not yield good results, so it is necessary to force the algorithm to push a little bit further. As a consequence, to evaluate the performance of the attacks, we will use two metrics : the success and transferability rates, for each distortion value. The first one measures the percentage of attacks which have been successful on the substitute NNC, while the second one measures the same percentage but for the oracle. The obtained results are given in Table 7.

γ	Metric	NT-Attack-Z (X=JSMA)					NT-Attack-F (X=JSMA)				
		X	WX	TX	M-X	M-WX	X	WX	TX	M-X	M-WX
1%	SR	65.9	75.4	78.6	37	40.7	75.3	77.1	80.1	77	77.4
	TR	43	46.5	48.2	31.8	34.2	48.1	44.8	50.3	45.4	43.4
2%	SR	81.2	89.4	93.1	55.4	56.8	88.6	91.3	94.5	94.9	95.3
	TR	56.6	59.2	63.4	50.1	49.5	62.1	58	64.1	56.5	58.8
3%	SR	88.5	95.5	97.7	68.9	67.4	94.4	95.8	98.6	99	99.2
	TR	65.1	67.2	70.2	58.8	59.2	69.3	64.1	70.7	64.5	65.3
4%	SR	92.9	97.1	99.2	77.7	74.7	97.4	98.3	99.5	100	100
	TR	69.2	71	75.3	68.5	65.1	73.9	67.5	74.8	69.9	69.5
5%	SR	96	98.7	99.9	83.5	79.5	98.5	99	100	100	100
	TR	71.9	73.6	77.9	72.7	68.4	76.3	71.1	77.2	72.3	72.1

Table 7: Success and transferability rates (SR & TR) in % for the black-box NT attacks on the 1, 000 to 2, 000 test samples of GTSRB for a distortion γ varying from 1% to 5%.

We can see in this table that in terms of success rate, the results are compatible with the white-box attacks results, meaning that M-WJSMA outperforms NT-TJSMA, which is better than NT-WJSMA which beats NT-JSMA. This is somewhat expected, because the attacks as performed on the substitute are merely white-box. More interestingly, concerning the transferability of the attacks, one can notice that for the Z attacks, the same hierarchy NT-TJSMA > NT-WJSMA > NT-JSMA is respected, while for the F attacks, NT-WJSMA is overall inferior to all the other attacks, and NT-TJSMA outperforms both NT-JSMA and M-JSMA.

Overall, NT-TJSMA is the best attack for black-box purposes, but the best variant (F or Z) depends on the distortion rate : NT-TJSMA-Z beats its counterpart NT-TJSMA-F for $\gamma = 4$ or 5 %. Finally, if one variant were to be chosen, it would be NT-TJSMA-F due to its speed and overall best transferability.

6 Conclusion

In this section, we summarise our main findings and also discuss the limitation of our work.

We have introduced WJSMA and TJSMA new probabilistic adversarial variants of JSMA for targeted and non-targeted misclassification of deep neural network classifiers.

Experiments in the targeted case have demonstrated, after analysing a large amount of images (more than 790,000 images), that our targeted attacks are more efficient and also faster than JSMA. It is important to recall the quite natural derivation of these attacks from a simple and classical log softmax reasoning

which has not been remarked before. Our attacks do not beat CW L_0 but have an important speed advantage highlighted in the paper. Therefore, for targeted L_0 misclassification, they offer substantial tools to test neural networks in real-time. This fact is supported by our fast implementation provided with the paper.

As a second contribution, we have introduced NT variants of WJSMA/TJSMA and have shown that they outperform the previous NT versions of JSMA. Through experiments on GTSRB, we remarked that the gap between our attacks and CW in L_0 average is reduced. Moreover, we obtained better success rate, while being at least 40 times faster than CW L_0 .

In the NT part of the paper, we did not compare our attacks with the one pixel attack [28]. Indeed, this approach is highly computational and we only claim an advantage in speed which is quite evident for us (see also the time evaluation in [15]). Also, we did not provide comparison with SparseFool [15] an effective NT L_0 attack because of the need to reimplement this attack with TensorFlow. On CIFAR-10, [15] found that crafting an example by SparseFool takes in average 0.34 and 0.69 second on two different neural networks. Our speed performances are very competitive to these values. Indeed, on GTSRB which has much more classes than CIFAR-10, our NT-TJSMA was able to craft an example in near 0.68 second in average (counting only successful images). Thus, regarding SparseFool, we first claim competitive results in speed. Second, our results obtained on LeNet-5 (more than 99.5% on a model similar to [15], see Section 5.1) are very close to [15] although we only run the attacks up to a limited maximum number of iterations contrary to [15].

Finally, we should mention that despite improving JSMA in different ways, like JSMA, our approach is still not scalable to large datasets. This is because of the high computational cost of saliency maps when the dimension of inputs becomes large. Our approach is therefore intended for "small" datasets such as those considered in the paper.

References

1. N Carlini and D Wagner. Towards evaluating the robustness of neural networks. *CoRR*, 1608.04644v2, 2017.
2. C Chio and D Freeman. Machine learning and security. *Oreilly*, 2018.
3. J. Deng, W. Dong, R. Socher, L. Li, Kai Li, and Li Fei-Fei. Imagenet: A large-scale hierarchical image database. In *2009 IEEE Conference on Computer Vision and Pattern Recognition*, pages 248–255, 2009.
4. Alessandro Erba, Riccardo Taormina, Stefano Galelli, Marcello Pogliani, Michele Carminati, Stefano Zanero, and Nils Ole Tippenhauer. Real-time Evasion Attacks with Physical Constraints on Deep Learning-based Anomaly Detectors in Industrial Control Systems. *arXiv e-prints*, page arXiv:1907.07487, July 2019.

5. Kevin Eykholt, Ivan Evtimov, Earlene Fernandes, Bo Li, Amir Rahmati, Chaowei Xiao, Atul Prakash, Tadayoshi Kohno, and Dawn Song. Robust physical-world attacks on deep learning visual classification. In *2018 IEEE Conference on Computer Vision and Pattern Recognition, CVPR 2018, Salt Lake City, UT, USA, June 18-22, 2018*, pages 1625–1634, 2018.
6. Yuan Gong, Boyang Li, Christian Poellabauer, and Yiyu Shi. Real-Time Adversarial Attacks. *arXiv e-prints*, page arXiv:1905.13399, May 2019.
7. I J Goodfellow, J Shlens, and C Szegedy. Explaining and harnessing adversarial examples. *ICLR*, 1412.6572v3, 2015.
8. Alex Krizhevsky, Vinod Nair, and Geoffrey Hinton. Cifar-10 (canadian institute for advanced research).
9. Alex Krizhevsky, Ilya Sutskever, and Geoffrey E. Hinton. Imagenet classification with deep convolutional neural networks. In *Advances in Neural Information Processing Systems*, page 2012.
10. A Kurabin, IJ Goodfellow, and S Bengio. Adversarial examples in the physical world. *ICLR*, 1607.02533v4, 2017.
11. Yann Lecun, Léon Bottou, Yoshua Bengio, and Patrick Haffner. Gradient-based learning applied to document recognition. In *Proceedings of the IEEE*, pages 2278–2324, 1998.
12. Yann LeCun and Corinna Cortes. MNIST handwritten digit database. 2010.
13. Jieyu Lin, Kristina Dzeroska, Sai Qian Zhang, Alberto Leon-Garcia, and Nicolas Papernot. On the robustness of cooperative multi-agent reinforcement learning. *ArXiv*, abs/2003.03722, 2020.
14. A Madry, A Makelov, L Schmidt, D Tsipras, and A Vladu. Towards deep learning models resistant to adversarial attacks. 1706.06083v3, 2017.
15. Apostolos Modas, Seyed-Mohsen Moosavi-Dezfooli, and Pascal Frossard. Sparsefool: A few pixels make a big difference. In *IEEE Conference on Computer Vision and Pattern Recognition, CVPR 2019, Long Beach, CA, USA, June 16-20, 2019*, pages 9087–9096. Computer Vision Foundation / IEEE, 2019.
16. S-M Moosavi-Dezfooli, A Fawzi, and P Frossard. Deepfool : a simple and accurate method to fool deep neural networks. *CoRR*, 1511.04599, 2015.
17. Seyed-Mohsen Moosavi-Dezfooli, Alhussein Fawzi, Omar Fawzi, and Pascal Frossard. Universal adversarial perturbations. In *2017 IEEE Conference on Computer Vision and Pattern Recognition, CVPR 2017, Honolulu, HI, USA, July 21-26, 2017*, pages 86–94, 2017.
18. N Papernot, P McDaniel, S Jha, M Fredrikson, Z Berkay Celik, , and A Swami. The limitations of deep learning in adversarial settings. *IEEE*, 1511.07528v1, 2015.
19. Nicolas Papernot, Fartash Faghri, Nicholas Carlini, Ian J. Goodfellow, Reuben Feinman, A. Kurakin, Cihang Xie, Yash Sharma, Tom H. Brown, Aurko Roy, Alexander Matyasko, Vahid Behzadan, Karen Hambarzumyan, Zhishuai Zhang, Yi-Lin Juang, Zhi Li, Ryan Sheatsley, Abhibhav Garg, Jonathan Uesato, Willi Gierke, Yinpeng Dong, David Berthelot, Paul N. J. Hendricks, Jonas Rauber, Rujun Long, and Patrick D. McDaniel. Technical report on the cleverhans v2.1.0 adversarial examples library. 2016.
20. Nicolas Papernot, Patrick D. McDaniel, Ian J. Goodfellow, Somesh Jha, Z. Berkay Celik, and Ananthram Swami. Practical black-box attacks against deep learning systems using adversarial examples. *CoRR*, abs/1602.02697, 2016.
21. Nicolas Papernot, Shuang Song, Ilya Mironov, Ananth Raghunathan, Kunal Talwar, and Úlfar Erlingsson. Scalable private learning with PATE. *CoRR*, abs/1802.08908, 2018.
22. A Parisi. Hands-on artificial intelligence for cybersecurity. *Packt Publishing*, 2019.
23. Kamalakanta Sethi, Sai Edupuganti, Rahul Kumar, Padmalochan Bera, and Y. Madhav. A context-aware robust intrusion detection system: a reinforcement learning-based approach. *International Journal of Information Security*, 12 2019.

24. Chawin Sitawarin, Arjun Nitin Bhagoji, Arsalan Mosenia, Mung Chiang, and Prateek Mittal. DARTS: deceiving autonomous cars with toxic signs. *CoRR*, abs/1802.06430, 2018.
25. Liwei Song, Reza Shokri, and Prateek Mittal. Privacy risks of securing machine learning models against adversarial examples. In *Proceedings of the 2019 ACM SIGSAC Conference on Computer and Communications Security, CCS 2019, London, UK, November 11-15, 2019*, pages 241–257, 2019.
26. J. Stalkamp, M. Schlipf, J. Salmen, and C. Igel. Man vs. computer: Benchmarking machine learning algorithms for traffic sign recognition. *Neural Networks*, (0):–, 2012.
27. J. Su, D. V. Vargas, and K. Sakurai. One pixel attack for fooling deep neural networks. *IEEE Transactions on Evolutionary Computation*, 23(5):828–841, 2019.
28. Jiawei Su, Danilo Vasconcellos Vargas, and Kouichi Sakurai. One pixel attack for fooling deep neural networks. *IEEE Trans. Evolutionary Computation*, 23(5):828–841, 2019.
29. R Wiyatno and A Xu. Maximal jacobian-based saliency map attack. 1808.07945v1, 2018.

7 Appendix

Architectures of the deep NNCs.

Table 8: LeNet-5 architecture

Layer	Parameters
Input Layer	size: (28×28)
Conv2D	kernel size: (5×5) , 20 kernels, no stride
ReLu	
MaxPooling2D	kernel size: (2×2) , stride: (2×2)
Conv2D	kernel size: (5×5) , 50 kernels, no stride
ReLu	
MaxPooling2D	kernel size: (2×2) , stride: (2×2)
Flatten	
Dense	size: 500
ReLu	
Dense	size: number of classes (10 for MNIST)
Softmax	

Table 9: Architecture of the used NNC on CIFAR-10

Layer	Parameters
Input Layer	size: (32×32)
Conv2D	kernel size: (3×3) , 64 kernels, no stride
ReLu	
Conv2D	kernel size: (3×3) , 128 kernels, no stride
ReLu	
MaxPooling2D	kernel size: (2×2) , stride: (2×2)
Conv2D	kernel size: (3×3) , 128 kernels, no stride
ReLu	
Conv2D	kernel size: (3×3) , 256 kernels, no stride
ReLu	
MaxPooling2D	kernel size: (2×2) , stride: (2×2)
Conv2D	kernel size: (3×3) , 256 kernels, no stride
ReLu	
Conv2D	kernel size: (3×3) , 512 kernels, no stride
ReLu	
MaxPooling2D	kernel size: (2×2) , stride: (2×2)
Conv2D	kernel size: (3×3) , 10 kernels, no stride
GlobalAveragePooling	kernel size: (2×2) , stride: (2×2)
Softmax	

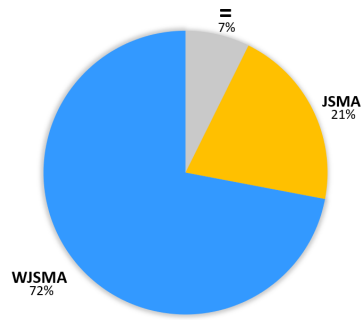
Table 10: Architecture of the used NNC on GTSRB

Layer	Parameters
Input Layer	size: (32×32)
Conv2D	kernel size: (5×5) , 64 kernels,no stride
ReLu	
MaxPooling2D	kernel size: (3×3) , stride: (2×2)
Conv2D	kernel size: (5×5) , 64 kernels,no stride
ReLu	
MaxPooling2D	kernel size: (3×3) , stride: (2×2)
Flatten	
Dense	size: 384
ReLu	
Dense	size: 192
ReLu	
Dense	size: 43
Softmax	

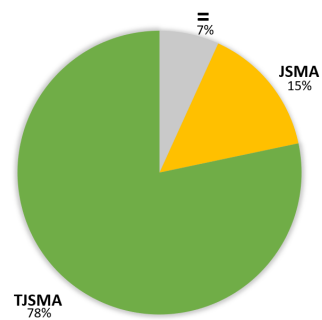
Table 11: Architecture of the used substitute NNC on GTSRB

Layer	Parameters
Input Layer	size: $(32 \times 32 \times 3)$
Conv2D	kernel size: (3×3) , 16 kernels,no stride
ReLu	
MaxPooling2D	kernel size: (2×2) , stride: (2×2)
Conv2D	kernel size: (3×3) , 32 kernels,no stride
ReLu	
MaxPooling2D	kernel size: (2×2) , stride: (2×2)
Conv2D	kernel size: (3×3) , 64 kernels,no stride
ReLu	
Flatten	
Dense	size: 43
Softmax	

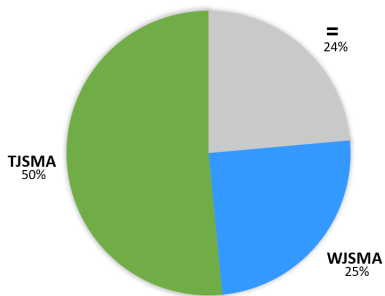
Pairwise dominance.



(a) WJSMA vs JSMA



(b) TJSMA vs JSMA



(c) TJSMA vs WJSMA

Fig. 6: Pairwise dominance on MNIST (= corresponds to samples with the same number of iterations by the attacks including when both attacks fail).

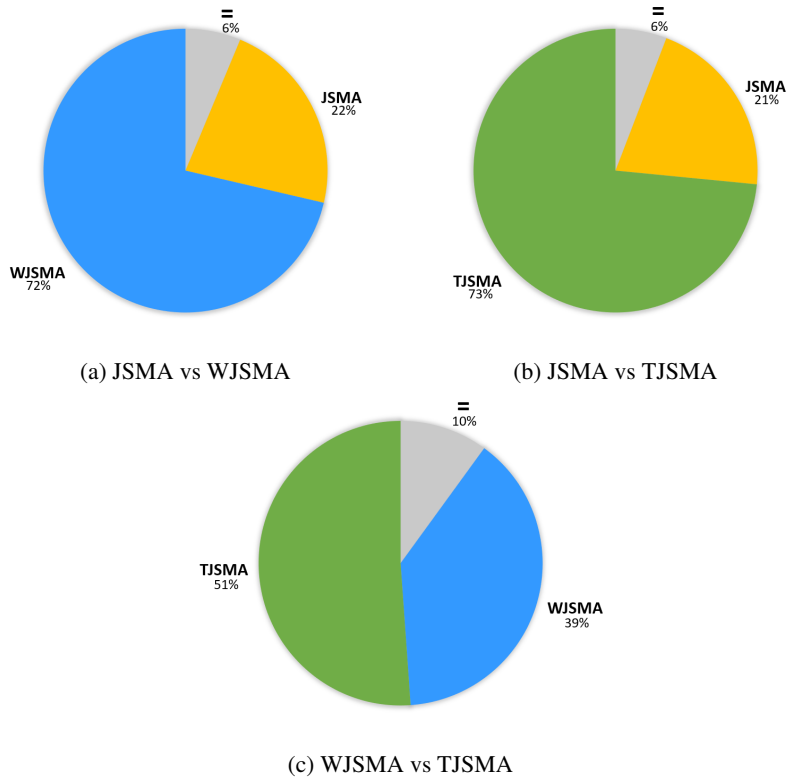


Fig. 7: Pairwise dominance on CIFAR-10 (= has the same significance as before).

Further analysis of the results obtained on MNIST reveals that, even for examples where JSMA is better than WJSMA or TJSMA, in average, less than 10 more components are changed by WJSMA or TJSMA, whereas JSMA changes more than 17 more components in average when it is dominated by WJSMA or TJSMA. A similar gap can be remarked in CIFAR-10.